J. Membrane Biol. 148, 193–202 (1995)

The Journal of
Membrane
Biology

Rapid Desensitization of $\alpha_1\beta_1$ $GABA_A$ Receptors Expressed in Sf9 Cells under Optimized Conditions

B. Birnir, M.L. Tierney, N.P. Pillai, G.B. Cox, P.W. Gage

John Curtin School of Medical Research, Australian National University, P.O. Box 334, Canberra, ACT, 2601, Australia

Received: 17 May 1995/Revised: 8 August 1995

Abstract. α_1 and β_1 subunits of human $GABA_A$ receptors were expressed in Sf9 cells using the Sf9-baculovirus system. Better expression was obtained by manipulating the system. Cell growth phase at the time of infection determined the practical range of virus titre, the period postinfection during which cells were useful for signal detection and the maximal current obtained. Cells in the early exponential phase were relatively insensitive to multiplicity of infection (MOI) whereas cells in the mid- to late-exponential phase were highly dependent on MOI and they responded with the largest Cl^- current generated by GABA. Channels activated by GABA were chloride-selective. Half the maximum peak whole-cell current was obtained with 11 μM GABA. The time course of Cl^- currents activated by saturating GABA concentrations in cells infected with $\alpha_1\beta_1$-recombinant viruses was examined employing a rapid perfusion system which allowed whole-cell solution exchange in less than 1 msec. The current decay could be fitted by 3 to 4 exponentials for the first 8 sec. The initial fast current decrease had a time constant of about 23 msec. No voltage dependence of time constants was detected but the whole-cell *IV* relation showed outward rectification. Currents were depressed by bicuculline, penicillin and picrotoxin and potentiated by pentobarbitone.

Key words: Baculovirus — Expression — Ion channel — Desensitization — Patch clamp — Rapid perfusion

Introduction

The $GABA_A$ receptor when activated by GABA (γ-aminobutyric acid) forms a Cl^- channel that mediates the rapid inhibition of excitatory synaptic transmission in central nervous systems. It has also been shown to be of functional importance in some peripheral tissues (Erdo & Wolff, 1990). Many different subunits have been cloned. They can associate in various combinations and provide the potential for functionally diverse receptors which may be the cause of the complex pharmacological profile of $GABA_A$ receptors observed in central nervous systems (Sivilotti & Nistri, 1991; Burt & Kamatchi, 1991; Zorumski & Isenberg, 1991).

We have expressed the α_1 and β_1 subunits of the human $GABA_A$ receptor in the baculovirus-Sf9 system. This system has been used in recent years to express membrane proteins including some ion channels (Klaiber et al., 1990; Kawamoto, Onishi & Hattori, 1991; Atkinson et al., 1992; Birnir et al., 1992; Carter, Thomsen & Im, 1992; Cascio et al., 1993). It appears to have post-translational modification mechanisms and transport systems similar to those of higher eukaryotic systems (Miller, 1988). The Sf9 cells are derived from ovarian cells of *Spodoptera frugiperda* and are capable of high expression of foreign proteins. They are spherical, 10 to 15 μm in diameter, and a high resistance seal is readily formed between a patch pipette and the cell membrane. These properties make the cells very suitable for studies of ion channel function using the patch clamp technique.

In this study, we have used the Sf9 preparation to characterize functional properties of "wild type" receptors so that we can later determine effects of selected mutations in either, or both subunits, of the human $\alpha_1\beta_1$ $GABA_A$ receptor. We have established conditions which ensured that 95% or more of the cells were infected and have defined parameters important for determining the expression level of functional $GABA_A$ receptors. The time course of the current response to GABA was examined by employing a rapid perfusion technique which enabled exposure of the whole cell surface to

Correspondence to: B. Birnir

GABA in less than a millisecond. This allowed detection of an early current decay with a time constant of about 23 msec.

Materials and Methods

Plasmid Construction

All methods for DNA manipulation were based on standard procedures (Sambrook, Fritsch & Maniatis, 1989). Oligonucleotide-directed mutagenesis was conducted according to the phosphorothioate technique of Taylor et al. (1985) using an Amersham Sculptor™ in vitro mutagenesis kit (RPN 1526). The cDNAs encoding α_1 and β_1 subunits of the $GABA_A$ receptor along with their signal sequences were subcloned from M13 constructs (obtained from Dr. P. Schofield, Garvan Institute of Medical Research, Sydney, Australia). The α_1 cDNA described in a previous publication (Birnir et al., 1992) contained two point mutations; an isoleucine to valine change at position 121 (numbering according to the mature protein sequence) and isoleucine to phenylalanine at position 290. These mutations were corrected and α_1 and β_1 cDNAs subcloned into the dual promoter baculovirus expression vector pAcUW31 (Clontech) using introduced compatible restriction sites. The α_1 protein was expressed under the p10 promoter and the β_1 protein under the polyhedrin promoter. Plasmids containing both the α_1 and β_1 cDNAs or either the α_1 or β_1 cDNA were named αβpAc, αpAc and βpAc, respectively. The authenticity of each plasmid was verified by sequencing of the insert cDNAs. Site specific mutations in the α_1 and β_1 cDNA were constructed in their respective M13 phage derivatives using the "Oligonucleotide directed in vitro mutagenesis system" from Amersham. The presence of the mutation was confirmed by DNA sequencing.

Cell Culture

Techniques for general handling of Sf9 cells, generating high titre viral stock and optimising protein production were derived from King and Possee (1992), Licari and Bailey (1991) and Summers and Smith (1988). The cells were grown in spinner cultures (50 rounds/min, Bellco spinner flasks, 25 ± 1°C) in insect culture medium (TNM-FH) composed of Graces' insect medium (Sigma), 4.0 g/l yeastolate (Gibco), 3.3 g/l lactalbumin (Gibco) and supplemented with 10% fetal bovine serum (CSL, Sydney, NSW, Australia) at pH 6.2 and normal osmolality of 330 mosmoles l^{-1}. New cultures were started at least every 3 months with thawed cells of low passage number. Cells used for cotransfection, the production of high titre viral supernatant and the plaque and titre assays were taken from cultures growing at 5 to 7×10^5 cells/ml. For optimum protein expression, cells were infected at 30 plaque-forming units/cell (pfu/cell) (multiplicity of infection (MOI) = 30). All incubations were carried out at 25°C and viral supernatant was stored at 4°C.

Viral Infections of Monolayers

Monolayers were prepared by seeding cells into flasks/plates and rocked (10/min) for 10 min at room temperature (RT, 19–22°C). This procedure ensured even distribution of the cells forming the monolayer. The TNM-FH medium was then replaced with enough virus inoculum to cover the cells. After 90 min at RT on the rocking platform the viral supernatant was removed, complete medium added and the cells incubated.

Generation and Isolation of Recombinant Viruses

The transfer vectors were purified using CsCl gradient centrifugation. The method of lipofection (Felgner, Gadek & Holm, 1987), was used to cotransfect Sf9 cells with linearized viral DNA and plasmid DNA. Briefly, 0.5 ng plasmid DNA and 5 µl Bsu-36I digested Bakpak 6 viral DNA (Clontech) were mixed with 50 µg lipofectin (Clontech). After 15 min, the mixture was added to a monolayer of 1.5×10^6 cells in 1.5 ml serum-free TNM-FH medium in 35 mm^2 plates and incubated for 5 hr. 1.5 ml of complete medium was then added to the mixture and the plates incubated. After 72 hr the viral supernatant was collected, centrifuged at 1,000 × *g* for 5 min and stored. In order to isolate recombinant viruses the supernatant was diluted to 10^{-2} and 10^{-3} with serum-free TNM-FH medium and 1.5×10^6 cells in 60 mm^2 plates infected for 90 min. The virus inoculum was then removed and the cells covered with 4 ml of complete medium containing 1% SeaPlaque low-melt agarose (FMC, Rockland, ME). When the agarose had set, 1 ml of TNM-FH medium was added. Recombinant plaques were isolated after 5–7 days, added to 1 ml of serum-free TNM-FH medium and stored for a minimum of 24 hr at 4°C before being used to produce recombinant viral supernatant. No further plaque purification was needed.

Production of High-Titre Viral Stock

25 cm^2 tissue culture flasks were seeded with 1.5×10^6 cells and infected with the 1 ml containing the isolated recombinant plaque. After 90 min, virus inoculum was removed and 5 ml complete medium added. Cells were incubated for 6 days and viral supernatant collected. The supernatant was centrifuged at 1,000 × *g* for 5 min and stored. The end point titration assay (King & Possee, 1992) was used to titre the supernatant which ranged from 10^6 to 10^8 pfu/ml. In order to make a larger volume of high titre viral stock, a 50 or 100 ml spinner flask was seeded at a cell density of 5×10^5 cells/ml with cells in the early exponential phase ($5–6 \cdot 10^5$ cells/ml). The culture was infected with the recombinant virus at an MOI of 0.06 to 0.2, grown for 6 days and then stored overnight at 4°C. The supernatant was centrifuged at 1,000 × g for 5 min and stored. The viral supernatant was titrated and commonly ranged from 10^8 to 10^9 pfu/ml. Recombinant viruses carrying α_1 and β_1 cDNAs or either α_1 or β_1 cDNA were named αβpAc, αpAc and βpAc viruses, respectively.

SDS Polyacrylamide Gel Electrophoresis and Western Blotting

1×10^5 cells in a monolayer were infected at MOI of 1, 10 or 30 according to standard procedure. Forty-eight hours postinfection, cells were resuspended in complete medium and centrifuged. The cells were washed twice with phosphate-buffered saline before being solubilized in 40 µl reduced sample buffer (BioRad). Electrophoresis was according to the method of Laemmli (1970). A 10.5% SDS polyacrylamide gel was loaded with 20 µl of sample, proteins separated and transferred to nitrocellulose (Towbin, Staehelin & Gordon, 1979). After blocking in milk powder, the nitrocellulose was incubated in α_1-specific monoclonal antibody bd24 (gift from H. Möhler, University of Zürich, Zürich, Switzerland) (Haring et al., 1985; Ewert et al., 1990). The bd24 antibody was diluted 1/30 in Tris-saline and immunodetection was by Enhanced Chemiluminescence (Amersham).

Recording Currents

Currents were recorded from Sf9 cells using standard whole-cell, tight-seal recording techniques (Hamill et al., 1981). Infection and incuba-

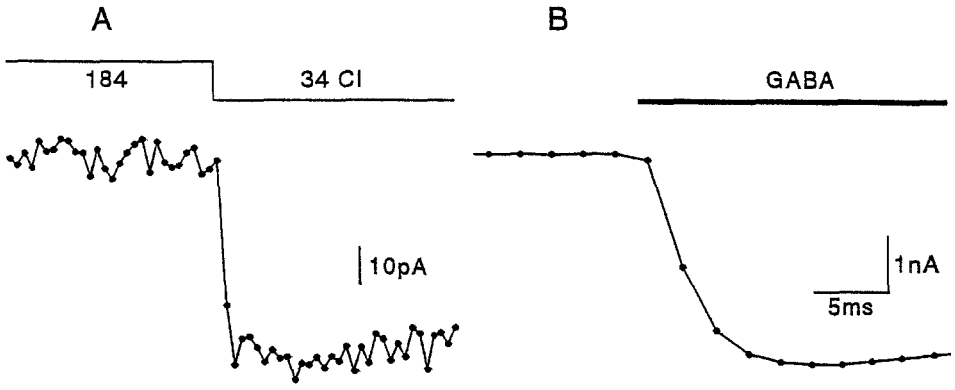

Fig. 1. (*A*) Rate of solution change across the surface of a cell. Current was recorded in the whole-cell mode at holding potential of 0 mV. The cell was initially exposed to 184 mM Cl^- and then rapidly to a 34 mM Cl^- extracellular solution. Iso-osmolality and $[Na^+]$ was maintained by replacing 150 mM NaCl with 150 mM NaGluconate. Data points are at 0.5 msec intervals. The time for the current to increase from 10 to 90% of the steady-state value was 0.5 msec. (*B*) Whole-cell current activated by 10 mM GABA at –40 mV holding potential. Data points are at 2 msec intervals. The current reached 90% of the peak current value in less than 5 msec.

tion of cells to be used for electrical measurements were carried out in 96 well plates according to routine procedures (*see* section on infections of monolayers). Cells were used 28 to 58 hr after infection. Patch electrodes were made from borosilicate glass (GC15F-15, Clark Electromedical instruments, Reading, UK) and had a resistance of 5 to 10 MΩ after fire-polishing and filling with pipette solution. The ground electrode was a 3M KCl agar bridge connected to a chlorided silver wire. Current was monitored with a current-to-voltage converter (Axopatch 200, Axon Instruments, Foster City, CA) using series resistance compensation. Cells were continuously perfused with bath solution (2–4 ml/min) containing either (mM): 30 KCl, 122 NaCl, 7 $CaCl_2$, 11 $MgCl_2$, 11 $MgSO_4$, 4 $NaHCO_3$, 7 NaH_2PO_4, pH 6.2 (345 mosmoles/l) or 180 NaCl, 1 $CaCl_2$, 1 $MgCl_2$, 10 MES (2-[N-Morpholino]ethanesulfonic acid) pH 6.2 (330 mosmoles/l). Similar results were obtained in the two bath solutions. In some experiments (specified in figure legends) Cl^- was replaced by gluconate resulting in a final chloride concentration of 34 mM in the bath solution. Pipettes were filled with a solution containing (mM): 180 NaCl, 1 $CaCl_2$, 1 $MgCl_2$, 5 EGTA, 10 TES (N-tris[Hydroxy]methyl-2-aminoethanesulfonic acid) pH 7.2 and usually 4 ATP (335 mosmoles/l) unless otherwise specified. Experiments were done at room temperature (19 to 22°C).

Applying GABA and Drugs

GABA and other drugs were dissolved in the bath solution and rapidly applied to cells by gravity feed through stainless steel delivery tubes that had an internal diameter of 200 to 300 μm. After establishing whole-cell recording, the cell was lifted off the glass plate and positioned at the center of the orifice of a delivery tube no further than 350 μm away. Flow from the drug delivery was turned on and off either manually with a tap or remotely using a solenoid valve. The rate of the solution exchange was highly dependent on the bath flow. For rapid solution changes, the flow rate in a 1 ml bath was maintained at 20 ml/min and flow was laminar. The rate of change of solution over the cell surface obtained with this technique was monitored by recording the change in the whole cell current when a new solution was applied to the surface of the cell, as illustrated in Fig. 1*A*. In this case, the bath solution contained 184 mM Cl^-. A jet of solution containing 34 mM Cl^- switched through the tube caused an inward current that reached a plateau in less than a millisecond. The time for the current to increase from 10 to 90% of the final steady current was approximately 0.5 msec. When GABA was applied to cells, currents normally reached a peak more slowly, as illustrated in Fig. 1*B*.

Results

Expression and Assembly of Receptors

The effects of cell growth status, MOI and time postinfection on the level of expression were examined. Typical growth curves for Sf9 cells are shown in Fig. 2. Each curve shows results from four spinners grown under identical conditions over a period of 3 weeks. During 3 months in spinners, the cells can from time to time grow according to one or the other growth curve. This variability in cell growth rate was not expected and we have no explanation for it at this time. The curves can be divided into exponential and stationary phases. The stationary phase was defined as starting when the cell density reached about 2×10^6 cells/ml. For cell viability, it was essential that the stationary growth phase was attained at least every second week and variations in medium osmolality were minimized. Cells grew and expressed heterologous protein when the osmolality ranged from 330 to 380 mosmoles/l, provided they were adjusted to any change in the medium they were exposed to. At osmolalities lower than 330 or higher than 380 mosmoles/l protein production decreased and cells eventually died. For both the slower growing and the faster growing cultures it was the growth status of the cells that determined whether they could be used to express foreign protein ($5–18 \times 10^5$ cells/ml) or to produce viral stock ($5–7 \times 10^5$ cells/ml). There was no detectable difference in the final product between the two cultures as long as the correct cell density was used. Therefore, in

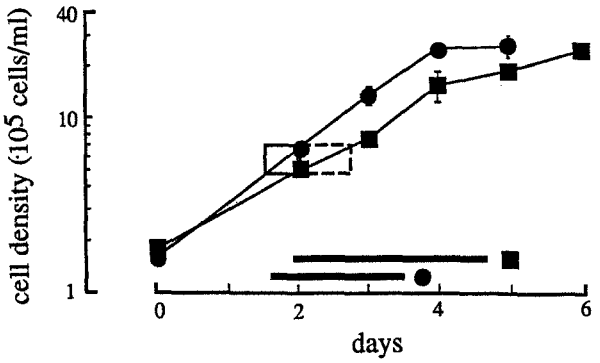

Fig. 2. Sf9 cell growth curves. Cell density (ordinate) is plotted against days in culture after a culture was diluted down to 1.5 ± 0.5 cells/ml on day 0. Normally cell culture was allowed to attain the stationary phase (starting at about 2×10^6 cells/ml) before being diluted down. Both curves show the averages of four spinner cultures grown under identical conditions for three weeks. The practical periods for making heterologous protein (horizontal bars) or viral supernatants (boxes) were determined by the cell growth status. For protein expression and viral production, cell density ranged from $5\text{-}18 \times 10^5$ and $5\text{-}7 \times 10^5$ cells/ml, respectively.

an attempt to have a population of cells with similar properties, a culture was not used unless it had been grown from $1.5 \pm 0.5 \times 10^5$ cells/ml (day 0, Fig. 2). When a culture had reached the appropriate density, cells were collected and used for experiments. In Fig. 2, the horizontal lines indicate the periods the cells were useful for protein production and the boxes when they were used to produce viral stock. In both cases the practical period lasts significantly longer in the slower growing culture.

The effect of MOI was examined by infecting cells at different stages of growth with αβpAc recombinant virus at a MOI of 1, 10 and 30 (Fig. 3*A*). We examined cells in the early- (5×10^5 cells/ml), mid- (13×10^5 cells/ml) and late- (18×10^5 cells/ml) exponential growth phase and early- (25×10^5 cells/ml) and late- (35×10^5 cells/ml) stationary phase for their ability to produce the α_1 protein. Protein production was scored 48-hr postinfection according to the intensity of protein bands detected on Western blots using the α_1-specific monoclonal antibody bd24. When cells were infected during the early-exponential growth phase, protein expression was high and relatively independent of MOI. During the mid- and late-exponential phases, protein expression became dependent on MOI and dropped sharply from MOI of 10 to MOI of 1. In the stationary phase (25 and 35×10^5 cells/ml), α_1 expression was significantly less than during the exponential phase.

Conditions affecting the whole-cell current amplitude generated by GABA were examined. The influence of cell growth status at the time of infection and the time postinfection experiments were performed is shown in Fig. 3*B*. The cells were infected at MOI of 30 ensuring that at least 95% of cells tested responded to GABA. Peak currents activated by application of 100 μM or 10 mM GABA at a holding potential of −40 mV were used as indicators of expression. The results were obtained from 57 cells. Noninfected cells showed no GABA activated current. Currents were recorded from 28 to 33 hr (light gray bars) or from 34 to 40 hr (dark gray bars) postinfection. When currents were recorded at 28–33 hr the largest currents were obtained from cells infected when growing at a density from $7\text{–}9 \times 10^5$ cells/ml (Fig. 3*B*). However, when currents were recorded at 34–40 hours, the largest currents were obtained from cells infected in the mid- to late-exponential growth phase (Fig. 3*B*) and this latter procedure gave the largest currents (up to 10 nA). Cell fragility increased with time postinfection, particularly cells infected in the early-exponential phase.

Background Current

In noninfected Sf9 cells, changes in membrane potential generated currents that reversed at 0 mV. The "background" conductance (given by $I/V\text{-}V_0$)), where I is the steady state current generated by voltage step V and V_0 is the potential at which $I = 0$) was normally in the range of 1–5 nS. The chloride component of the background current varied somewhat. When the cells were held at 0 mV and the Cl^- concentration in the extracellular solution was lowered from 184 to 34 mM Cl^- the average conductance in 23 cells was 2.7 ± 0.8 nS. The background conductance was affected by the osmolality of the bath and pipette solutions and the presence of divalent cations in the pipette solution. When the extracellular solution had an osmolarity lower than 310 mosmoles/l, the cells appeared swollen and the background conductance increased. Furthermore, in the absence of divalent cations in the pipette solution, the background conductance increased to more than 40 nS. For this reason, the osmolality of solutions was closely monitored and the intracellular solution always contained Ca^{2+} and Mg^{2+} (*see* Materials and Methods).

In cells infected with αβpAc recombinant viruses, the background current was similar to that in control cells. Current-voltage (*IV*) curves in infected cells before exposure to GABA were reasonably linear from −100 to +40 mV but occasionally showed slight outward rectification at more positive potentials. The slope of the *IV* curve at potentials more negative than +40 mV gave conductances of 1 to 5 nS in "good" cells under optimum conditions. In some cells the background conductance slowly decreased when the membrane was held at potentials more negative than −50 mV.

The Response to GABA

Noninfected Sf9 cells showed no response to GABA. Rapid, sustained application of 0.1–10 mM GABA to

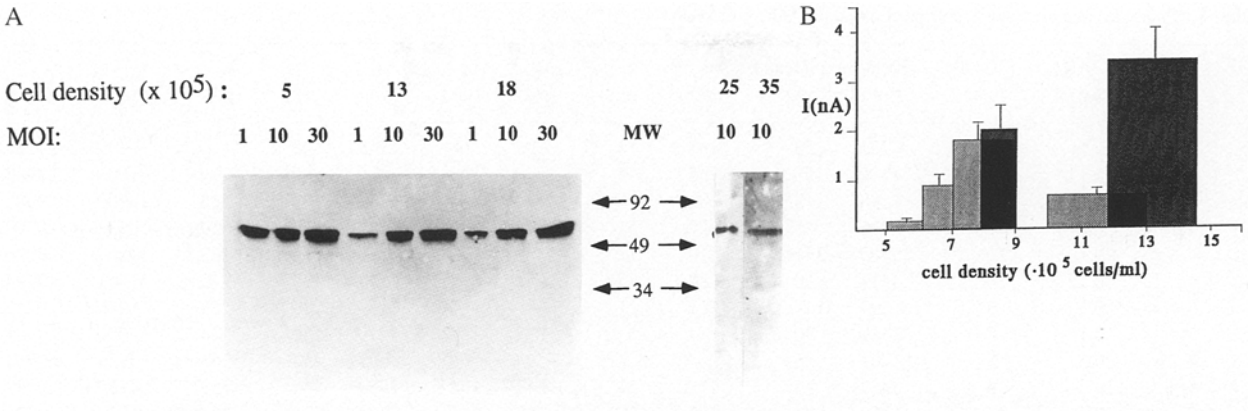

Fig. 3. Expression and assembly of receptors as a function of MOI, cell growth status and time postinfection. (*A*) Western blot at 48 hr postinfection using the α_1-specific monoclonal antibody bd24 to detect the presence of the glycosylated 56 kDa α_1 protein. 1×10^5 cells in the early- (5×10^5 cells/ml), mid- (13×10^5 cells/ml) and late- (18×10^5 cells/ml) exponential phase were infected at multiplicity of infection (MOI) of 1, 10 and 30 and cells in the early- (25×10^5 cells/ml) and late- (35×10^5 cells/ml) stationary phase at MOI of 10. The markers indicate molecular weights of 92, 99 and 34 kDa. (*B*) The relationship between the peak whole-cell Cl^- currents activated by saturating GABA concentrations (ordinate) and the cell density the cells were growing at, at the time of infection (abscissa). MOI was 30, [GABA] was 0.1 or 10 mM and the holding potential was –40 mV. Experiments were carried out 28–33 hr postinfection (light grey bars) or 34–40 hr postinfection (dark grey bars). The currents were recorded from 57 cells and each bar represents the mean ± 1 SEM of 4 or more cells.

infected cells gave a current that increased rapidly in amplitude and then decayed. A current generated by 10 mM GABA in an αβpAc-infected cell at a potential of –40 mV is shown in Fig. 4. (Although 10 mM gave no larger responses than 100 μM GABA the time-to-peak tended to be faster with the higher concentration (Table 1).) The rise time of the current (from 10 to 90% of the peak amplitude) was less than 5 msec. The decay of the current was complex but could generally be fitted up to about 8 s after the peak current with the sum of 3 or 4 exponentials with different time constants (using "Peak-fit," Jandel Scientific) according to Eq. 1:

$$I(t) = A_1\exp(-t/\tau_1) + A_2\exp(-t/\tau_2) + A_3\exp(-t/\tau_3) + A_4\exp(-t/\tau_4) + C \quad (1)$$

where A_i (*pA*) and τ_i (msec) are the initial amplitude and time constant of the "*i*"th component. This is illustrated for one cell in Fig. 4*B* where the decay was fitted by:

$$I(t)pA = 528\exp(-t/29) + 727\exp(-t/111) + 1789\exp(-t/456) + 330\exp(-t/2432) + 160$$

where *t* is time (msec) after the peak. The inset current shows the fast component of the decay at higher time resolution. The current response to 10 mM GABA at + 40 mV was similar (*not shown*). The current decay could be fitted with similar rate constants and there was no indication of voltage dependence of decay time constants. The rise times and decay time constants of responses to 100 μM and 10 mM GABA in 10 cells at a potential of –40 mV are listed in Table 1. It can be seen

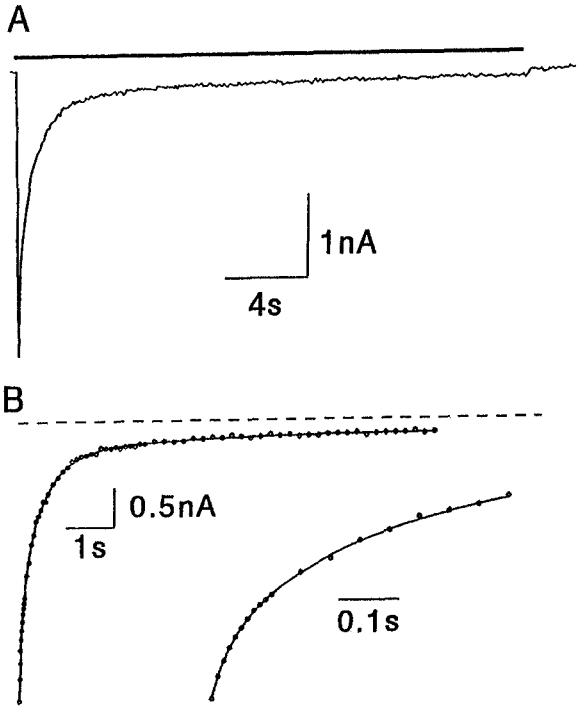

Fig. 4. Time course of whole-cell current activated by GABA. (*A*) Multiphasic current induced by 10 mM GABA applied during the time period indicated by the bar. The membrane potential was clamped at –40 mV. Downward deflection represents inward current. (*B*) The time course of desensitization of the current trace in (*A*) was fitted by Eq. 1. The four decay time constants were 29, 111, 456 and 2432 msec and the constant (plateau) current was 160 pA. The current traces at the two different time scales demonstrate the goodness of the fit during both the early (0.1-sec time scale) and the latter phases of decay (1-sec time scale).

Table 1. Characteristics of whole-cell currents activated by GABA

Cell	Trace (sec)	[GABA] (mM)	10–90% (ms)	Peak (pA)	plateau (pA)	A_1 (pA)	τ_1 (ms)	A_2 (pA)	τ_2 (ms)	A_3 (pA)	τ_3 (ms)	A_4 (pA)	τ_4 (ms)	r^2
1	2	0.1	4	723	23	185	13	297	68	217	343			0.9968
2	2	0.1	6	1415	156	145	15	510	141	680	580	79	1000	0.9983
2	4	0.1	6	1588	13			89	81	1183	602	316	10000	0.9988
3	4.5	0.1	18	8975	5	827	51	1747	292	5349	618	1052	6677	0.9997
4	4	0.1	16	6683	341	10	11	2385	239	3556	632	732	10867	0.9996
4	4	0.1	8	4413	0	280	35	1654	393	1740	717	740	11561	0.9994
5	6	0.1	6	1392	147	11	21			1131	920	250	8946	0.9973
6	5	0.1	8	2389	30			883	112	1279	580	244	5000	0.9981
6	4	0.1	8	1701	6			544	66	893	454	263	3989	0.9964
6	5	10	6	3422	83	411	21	817	102	1834	464	359	4160	0.9988
7	5	10	4	1060	82	235	30	268	351	366	536	191	1755	0.9972
8	5	10	12	4300	165	1070	21	1895	98	1226	467			0.9979
9	5	10	4	1510	62	492	17	500	89	493	394	24	1000	0.9909
10	0.7	10	6	834	12	268	18	196	76	261	200	109	1000	0.9884
10	5	10	6	2020	39			93	100	1662	750	265	6121	0.9987
		n	15	15	15	11	11	14	14	15	15	13	13	
		avg	7.87	2828	78	358	23	848	158	1458	550	356	5544	
		SEM	1.12	591	23	95.1	3.35	195	28.9	341	43.9	80.3	1028	

Currents were recorded in 10 cells (column 1). In some cells, the same GABA concentration was repeated twice, in others the cell was exposed in turn to 2 different concentrations (column 3). Equation 1 was fitted to the decay of the currents for the times shown under "trace." The 10–90% rise times are shown in column 4.

that there was considerable variability between cells. It is possible that some variability in the rate of exposure of the whole of the cell surface to GABA may have contributed to the variation in rise times, and perhaps to the first, fast phase of the decay. However, this would not explain the differences in the slower phases of the decay. Even when GABA was reapplied to the same cell after a delay, the decays of the responses were often not identical (Table 1, cells 3, 5, 6, 7). The source of this variability is not known.

IV Relation and Chloride-selectivity

The current generated by GABA reversed close to 0 mV in symmetrical chloride solutions. The current generated by a ramp voltage command after exposure of a cell to 3 μM GABA is shown in Fig. 5*A* (the control current, generated by the same voltage ramp before exposure of the cell to GABA, has been subtracted). The significant outward rectification was normally observed in infected cells. Similar results were obtained when the GABA concentration was 10 or 100 μM. It can be seen that the voltage for zero current (null potential) was close to 0 mV. This null potential suggested that the current was a chloride current, but it could also have been a nonspecific cation current. However, when GABA was applied to cells held at 0 mV in the same extracellular solution except that the chloride concentration was lowered from 184 to 34 mM Cl^- at the same time so that there was an outward concentration gradient for Cl^- ions, there was an inward current that could only have been a chloride current. This is illustrated in a cell during application of 100 μM GABA and 34 mM Cl^- (Fig. 5*B*). As the inside and outside solutions always contained the same concentration of cations and the potential was 0 mV, the current generated by GABA must have been a chloride current. In the absence of GABA, application of 34 mM Cl^- solution to the same cell gave no detectable current.

Dose-response Relationship

A detectable current was generated by GABA at concentrations of 1 μM and above. Increasing the GABA concentration above 100 μM gave no significant increase in current amplitude. The relationship between peak amplitude of the current response to GABA recorded in 12 cells is plotted against GABA concentration in Fig. 6. To overcome the variability in the response to GABA from cell to cell, presumably due to differences in receptor density, current amplitude was normalized to the average amplitude of the current generated by 100 μM GABA in the same cell before and after exposure to the test concentration. The second response was used to test for stability of the GABA response. If it differed by more than 20% from the first, the observation was not used. The solid line through the points is a fit of the Hill equation:

$$I = I_{max} \cdot [GABA]^n / ((K_{0.5})^n + [GABA]^n) \quad (2)$$

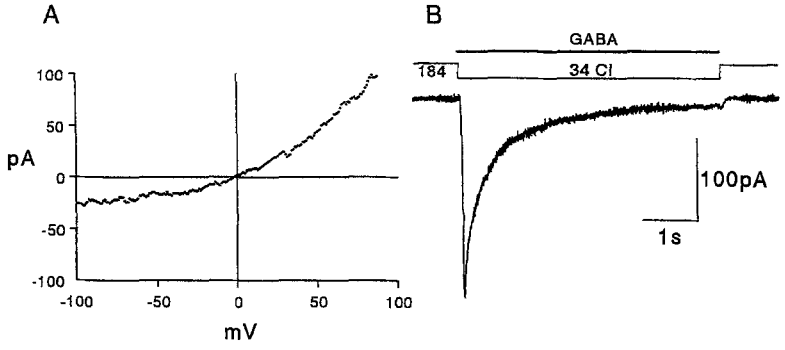

Fig. 5. (*A*) Current-voltage relation. Whole-cell currents activated by GABA show outward rectification. Currents were measured during a 1 sec voltage ramp from −100 to +100 mV during the plateau of the response to GABA. The current shown was obtained by subtracting the background current generated by the ramp in the absence of GABA from current induced by 3 μM GABA. (*B*) Current generated by GABA in asymmetrical [Cl^-] solution at a clamp potential of 0 mV. The pipette [Cl^-] was 184 mM. GABA (100 μM) applied in a solution containing 34 mM Cl^- generated an inward current that must have been a chloride current. In this cell in the absence of GABA the low Cl^- solution produced no detectable current.

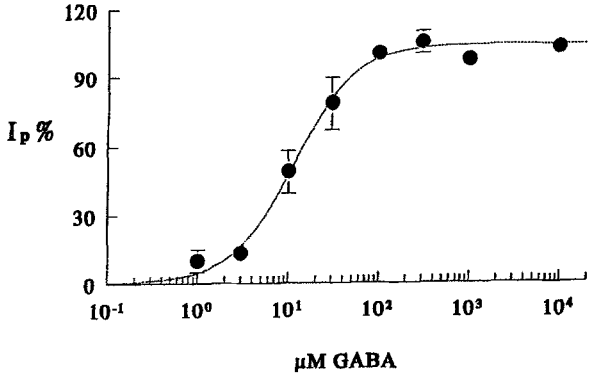

Fig. 6. Dose-response curve of whole-cell currents generated by GABA. In each cell, the peak currents elicited by various concentrations of GABA were normalized to that elicited by 100 μM GABA. Symbols show the mean ± 1SEM. The data were gathered from 12 cells at the holding potential of −40 mV. The activation curve was calculated by fitting the Hill equation (*see Results*) by nonlinear regression analysis to the data. The concentration of GABA that gave the half-maximal response was 11 μM and the Hill coefficient was 1.3.

to the data. The GABA concentration that gave half-maximal response ($K_{0.5}$) was 11 μM and the Hill coefficient (n) was 1.3.

Pharmacology

The GABA-gated Cl^- currents were inhibited by bicuculline, picrotoxin and penicillin and potentiated by pentobarbitone. 100 μM bicuculline blocked 84% ± 5.95% (mean ± 1SEM, n = 3) of the current evoked by 100 μM GABA. An example from one cell is shown in Fig. 7*A*. Penicillin (Fig. 7*B*) and picrotoxin (Fig. 7*C*) partially depressed the response to GABA. In 5 cells, 10 mM penicillin blocked 60% ± 3.5% (mean ± 1SEM) of the peak current induced by 100 μM GABA but 80% ± 8.1% (mean ± 8.2, n = 5) of the current integrated over the first 1–3 sec of the response. 100 μM picrotoxin, on the other hand, depressed the peak current activated by 100 μM GABA by 54% ± 0.94% (mean ± 1SEM, n = 8) but caused 88% ± 2.1% (mean ± 1SEM, n = 8) inhibition of the current integrated over the first 1–3 sec of the response. In both cases, the depression of the peak current was less than the overall inhibition of the response brought about by the time dependent attenuation of the current in the presence of the drug. In eight cells, 100 μM pentobarbitone potentiated the current response to 10 μM GABA as is illustrated in Fig. 7*D*. The peak current amplitude increased by 62% ± 1.3% (mean ± SEM). As expected, diazepam had no effect on the current evoked by GABA (*not shown*).

The Response to GABA of Mutated Receptors

We have made receptors carrying mutations in the second transmembrane region (M2) of the $GABA_A$ receptor subunits. Residues targeted for mutagenesis were threonine at position 267 in the α_1 subunit and the comparable threonine residue in the β_1 subunit at positon 262. Both were mutated to glutamine and the double mutated receptor, α_1(T267Q)β_1(T262Q), studied with respect to the rate and extent of desensitization of the GABA-activated Cl^- current. Representative currents generated by 10 mM GABA when applied to cells expressing either the mutant receptor or the wild type receptor are shown in Fig. 8. The membrane potential was −40 mV. It can be seen that both the fastest (τ_1) and the slowest (τ_4) time constants of the current decay observed for the wild-type receptor are absent in the mutated receptor. Furthermore, GABA application to a α_1(T267Q)β_1(T262Q)-pAc-infected cell generates no platau current and the current decays to baseline during the drug application.

Discussion

We have established conditions for optimal expression of $GABA_A$ receptor subunits in the baculovirus-Sf9 expression system. The small spherical cells, the low background current, high percentage of infected cells attainable, and the high level of expression possible make the

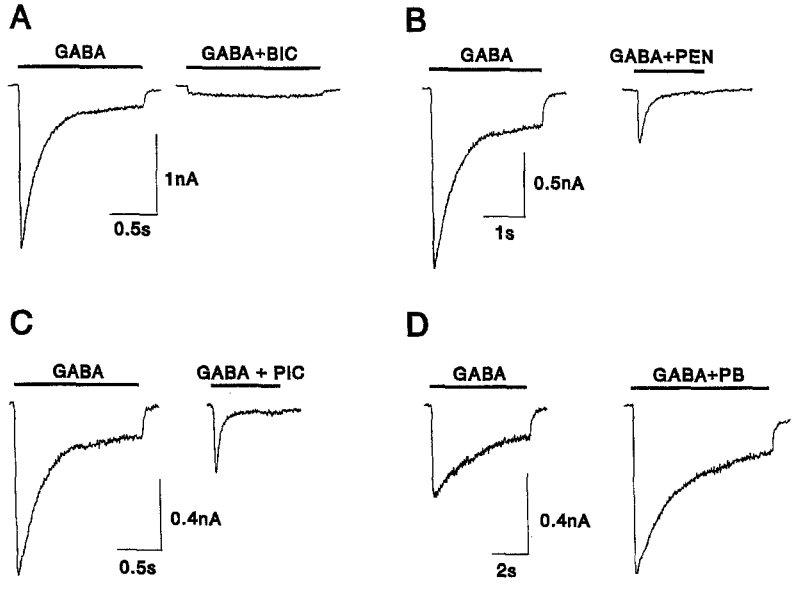

Fig. 7. Effects of drugs on whole-cell currents generated by GABA. Cl^- currents elicited by GABA alone were compared to currents activated by GABA in the presence of (*A*) 100 μM bicuculline (BIC), (*B*) 10 mM penicillin (PEN), (*C*) 100 μM picrotoxin (PIC) or (*D*) 100 μM pentobarbitone (PB). In *A*, *B*, and *C*, the GABA concentration was 100 μM and in *D* 10 μM. Drugs were applied during the time period indicated by the bar. Membrane potential was clamped at −40 mV.

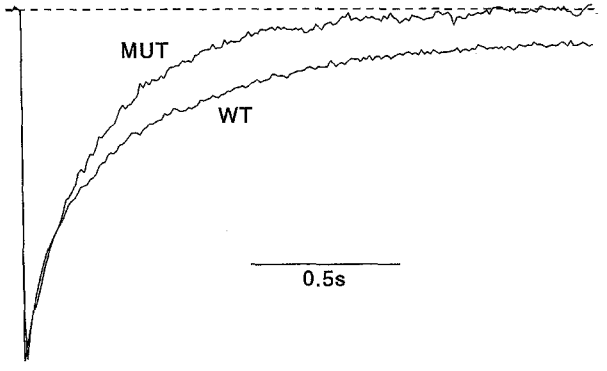

Fig. 8. Time course of whole-cell current activated by GABA in α_1(T267Q)β_1(T262Q) mutated receptor. During GABA application the current response of the mutated receptor (MUT) decayed to baseline. The peak current decay of the cell expressing the mutated receptor was scaled to the peak current amplitude of a cell expressing the wild type receptor (WT) to allow comparison of the time course of the current decay. In both cases, 10 mM GABA was present from the time of application. The membrane potential was clamped at −40 mV.

system a viable alternative to the more commonly used eukaryotic expression systems for studying ion channels (Blair et al., 1988; Verdoorn et al., 1990; Angelotti, Uhler & MacDonald, 1993*a*). To use the system effectively, it was essential to establish the cell growth curve since the expressed heterologous protein level is highly dependent on the cell's growth status when infected, as well as on the MOI. For this reason, spinner cultures are more practical than monolayers since cell growth (cells/ml) is easily monitored. Cells growing in the early-exponential phase should be used if virus titre is low or an early signal detection is desirable. On the other hand, in order to obtain maximal expression, cells in the mid- to late-exponential phase should be used.

The pharmacological profile of the expressed receptors was similar to that reported for $GABA_A$ receptors in other systems (Levitan et al., 1988; Akaike, Tokutomi & Ikemoto, 1990; Sigel et al., 1990; Twyman, Green & MacDonald, 1992; Porter et al., 1992; Yoon, Covey & Rothman, 1993). Bicuculline, penicillin and picrotoxin all reduced the current induced by GABA and pentobarbitone potentiated the response to GABA. Penicillin, picrotoxin and pentobarbitone all affected both the peak amplitude and the time course of the response. It is well established that penicillin and picrotoxin block $GABA_A$ single channel currents, but whether they affect the changes which lead to desensitization of the receptor remains to be established. The affinity ($K_{0.5}$) of the receptors for GABA was within the reported range ($K_{0.5}$: 1 to 13 μM) (Levitan et al., 1988; Sigel et al., 1990; Angelotti et al., 1993*a*; Krishek et al., 1994). In this study, we rapidly exchanged solutions around the Sf9 cells (Fig. 1) whereas most studies of whole-cell currents have used relatively slow application of GABA making it difficult to observe the initial fast current decay. Since $K_{0.5}$ values are determined from peak currents, variations may result from differences in the rate of drug application.

Part of the decline in the current generated by GABA could conceivably be due to a change in driving force on chloride ions because of a fall in intracellular chloride ion concentration (Akaike, Inomata & Tokutomi, 1987). However, it can be shown that currents such as that in Fig. 4 would cause very little change in driving force ($V - E_{Cl}$). In a small cell with a diameter of 10 μm, the current in Fig. 4, integrated over the time period GABA was applied and more than 3 nA at its peak, could cause a drop in $[Cl]_i$ from 184 to 147 mM if there were no replacement of Cl^- from the pipette. In symmetrical chloride solutions, E_{Cl} would change from 0

to −5.7 mV. This would decrease the driving force on chloride ions from −40 to −34.3 mV and cause a decrease in current of 14.3% at most. Other evidence indicates that the rate of decay of the currents was not being significantly contaminated by changes in $[Cl]_i$. (i) the decay time constants of currents were similar for large and small currents (Table 1). (ii) The current generated by GABA (3,10 or 100 μM) continued to reverse close to 0 mV late in the response to GABA (Fig. 5*A*) indicating that E_{Cl} had not changed significantly. (iii) There was no overshoot in currents when superfusion with GABA was stopped (e.g., Fig. 4).

In light of the flexibility of the Sf9-baculovirus system, it is useful for examining functional properties of ligand-gated receptors and the various processes which regulate and affect their function. It can be advantageous to examine the activation and desensitization of ligand-gated currents in intact cells as compared to cell patches. Transient modifications of receptors (i.e., phosphorylation) have been shown to affect these processes (Porter et al., 1990; Browning et al., 1990; Leidenheimer, Browning & Harris, 1991; Sigel, Baur & Malherbe, 1991; Kano & Konnerth, 1992; Moss et al., 1992; Agopyan, Tokutomi & Akaike, 1993; Angelotti, Uhler & MacDonald, 1993*b*; Lanius, Pasqualotto & Shaw, 1993; Krishek et al., 1994; McDonald & Moss, 1994) and desensitization of channels in outside-out patches can be different from that observed in whole-cell recordings (Frosch, Lipton & Dichter, 1992). There are varying reports on the rate and degree of desensitization of $GABA_A$ receptors. Electrophysiological studies commonly give desensitization time constants from hundreds of milliseconds to tens of seconds (Huguenard & Alger, 1986; Akaike, Inomata & Tokutomi, 1987; Levitan et al., 1988; Akaike, Tokutomi & Ikemoto, 1990; Verdoorn et al., 1990; Frosch et al., 1992; Geetha & Hess, 1992; Oh & Dichter, 1988; Yoon, 1994; Schönrock & Bormann, 1993; Krishek et al., 1994). In order to look for a fast phase of desensitization, receptor activation must be rapid requiring solution change around the cell/patch to be fast. This has been achieved for patches in less than 1 msec (Clements & Westbrook, 1991; Celentano & Wong, 1994) whereas whole-cell solution exchange is usually slower (about 10 msec or more; Bean, 1990; Vyklicky, Benveniste & Mayer, 1990; Geetha & Hess, 1992; Krishek et al., 1994). The small size and spherical shape of Sf9 cells allow rapid solution change around the cell (Fig. 1*A*). Celentano and Wong (1994) demonstrated rapid desensitization rate constants for $GABA_A$ receptors in outside-out patches from pyramidal cells in the CA1 region of guinea pig hippocampus (15, 207, and 1370 msec). These rate constants are of the same order as those we found in this study. In the CA1 region of the hippocampus, a variety of $GABA_A$ subunits have been reported (Laurie, Wisden & Seeburg, 1992) whereas the GABA receptors in the Sf9 cells can have contained only α_1 and β_1 subunits. It may be that desensitization of $GABA_A$ receptors is governed by the α or the β subunits or is independent of subunit composition. However, the relative contribution of the various phases to the overall process may differ among the different complexes.

Finally, we have characterized the amplitude and time course of currents generated by wild-type $\alpha_1\beta_1$ receptors activated by GABA in Sf9 cells, their affinity for GABA, and the effects of the drugs penicillin, picrotoxin, pentobarbitone and bicuculline. These will provide an essential "control" for evaluating the effects of mutations in the α_1 and/or β_1 subunits. Preliminary results indicate that significant changes are produced by single point mutations in the second transmembrane region of both subunits.

We are grateful to I. Woo and B. MacLachlan for their expert technical assistance and L. Hardy for secretarial assistance. This work was generously supported by: Sir Rutherford Robertson, Sir John Pround, The Raymond E. Purves Foundation, The James N. Kirby Foundation, C. H. Warman and the Bruce and Joy Reid Foundation.

References

Agopyan, N., Tokutomi, N., Akaike, N. 1993. Protein kinase A-mediated phosphorylation reduces only the fast desensitizing glycine current in acutely dissociated ventromedial hypothalamic neurons. *Neuroscience* **56:**605–615

Akaike, N., Inomata, N., Tokutomi, N. 1987. Contribution of chloride shifts to the fade of γ-aminobutyric acid-gated currents in frog dorsal root ganglion cells. *J. Physiol.* **391:**219–234

Akaike, N., Tokutomi, N., Ikemoto, Y. 1990. Augmentation of GABA-induced current in frog sensory neurons by pentobarbital. *Am. J. Physiol.* C452–C460

Angelotti, T.P., Uhler, M.D., MacDonald, R.L. 1993*a*. Assembly of $GABA_A$ receptor subunits: Analysis of transient single-cell expression utilizing a fluorescent substrate/marker gene technique. *J. Neurosci.* **13,4:**1418–1428

Angelotti, T.P., Uhler, M.D., MacDonald, R.L. 1993*b*. Enhancement of recombinant γ-aminobutyric acid type A receptor currents by chronic activation of cAMP-dependent protein kinase. *Mol. Pharmacol.* **44:**1202–1210

Atkinson, A.E., Bermudez, I., Darlison, M.G. 1992. Assembly of functional $GABA_A$ receptors in insect cells using baculovirus expression vectors. *NeuroReport* **3,7:**597–600

Bean, B.P. 1990. ATP-activated channels in rat and bullfrog sensory neurons: concentration dependence and kinetics. *J. Neurosci.* **10:**1–10

Birnir, B., Tierney, M.L., Howitt, S.M., Cox, G.B., Gage, P.W. 1992. A combination of human α_1 and β_1 subunits is required for formation of detectable GABA-activated chloride channels in Sf9 cells. *Proc. R. Soc. Lond. B* **250:**307–312

Blair, L.A.C., Levitan, E.S., Marshall, J., Dionne, V.E., Barnard, E.A. 1988. Single subunits of the $GABA_A$ receptor form ion channels with properties of the native receptor. *Science* **242:**577–579

Browning, M.D., Bureau, M., Dudek, E.M., Olsen, R.W. 1990. Protein kinase C and cAMP-dependent protein kinase phosphorylate the β subunit of the purified γ-aminobutyric acid A receptor. *Proc. Natl. Acad. Sci. USA* **87:**1315–1318

Burt, D.R., Kamatchi, G.L. 1991. $GABA_A$ receptor subtypes: from pharmacology to molecular biology. *FASEB J.* **5:**2916–2923

Carter, D.B., Thomsen, D.R., Im, W.B., et al., 1992. Functional expression of $GABA_A$ chloride channels and benzodiazepine binding sites in baculovirus infected insect cells. *Biotechnology* **10:**679–681

Cascio, M., Schoppa, N.E., Grodzicki, R.L., Sigworth, F.J., Fox, R.O. 1993. Functional expression and purification of a homomeric human α_1 glycine receptor in baculovirus-infected insect cells. *J. Biol. Chem.* **268:**22135–22142

Celentano, J.J., Wong, R.K.S. 1994. Multiphasic desensitization of the $GABA_A$-receptor in outside-out patches. *Biophys. J.* **66:**1039–1050

Clements, J.D., Westbrook, G.L. 1991. Activation kinetics reveal the number of glutamate and glycine binding sites on the N-methyl-D-aspartate receptor. *Neuron* **7:**605–613

Erdo, S.L. Wolff, J.R. 1990. Gamma-Aminobutyric acid outside the mammalian brain. *J. Neurochem.* **54:**363–372

Ewert, M., Shivers, B.D., Luddens, H., Möhler, H., Seeburg, P.H. 1990. Subunit selectivity and epitope characterization of mAbs directed against the $GABA_A$/benzodiazepine receptor. *J. Cell Biol.* **110:** 2043–2048

Felgner, P.L., Gadek, T.R., Holm, M. 1987. Lipofection: a highly efficient, lipid-mediated DNA-transfection procedure. *Proc. Natl. Acad. Sci. USA* **84:**7413–7417

Frosch, M.P., Lipton, S.A., Dichter, M.A. 1992. Desensitization of GABA-activated currents and channels in cultured cortical neurons. *J. Neurosci.* **12:**3042–3053

Geetha, N., Hess, G.P. 1992. On the mechanism of the γ-aminobutyric acid receptor in the mammalian (mouse) cerebral cortex. Chemicals Kinetic investigations with a 10-ms time resolution adapted to measurements of neuronal receptor function in single cells. *Biochemistry* **31:**5388–5499

Hamill, O.P., Marty, A., Neher, E., Sakmann, B., Sigworth, F.J. 1981. Improved patch-clamp techniques for high-resolution current recording from cells and cell-free membrane patches. *Pfluegers Arch.* **391:**85–100

Haring, P., Stahli, C., Schoch, P., Takacs, B., Staehelin, T., Möhler, H. 1985. Monoclonal antibodies reveal structural homogeneity of gamma-aminobutyric acid/benzodiazepine receptors in different brain areas. *Proc. Natl. Acad. Sci. USA* **82:**4837–4841

Huguenard, J.R., Alger, B.E. 1986. Whole-cell voltage-clamp study of the fading of GABA-activated currents in acutely dissociated hippocampal neurons. *J. Neurophysiol.* **56:**1–18

Kano, M., Konnerth, A. 1992. Potentiation of GABA-mediated currents by cAMP-dependent protein kinase. *NeuroReport* **3:**463–566

Kawamoto, S., Onishi, H., Hattori, S. 1991. Functional expression of the α_1 subunit of the ampa-selective glutamate receptor channel, using a baculovirus system. *Biochem. Biophys. Res. Commun.* **181:**756–763

King, L.A., Possee, R.D. 1992. The Baculovirus Expression System. A Laboratory Guide, Chapman & Hall, London

Klaiber, K., Williams, N., Roberts, T.M., Papazian, D.M., Jan, L.Y., Miller, C. 1990. Functional expression of *Shaker* K^+ channels in a baculovirus-infected insect cell line. *Neuron* **5:**221–226

Krishek, B.J., Xie, X., Blackstone, C., Huganir, R.L., Moss, S.J., Smart, T.G. 1994. Regulation of $GABA_A$ receptor function by protein kinase C phosphorylation. *Neuron* **12:**1061–1095

Laemmli, U.K. 1970. Cleavage of structural proteins during the assembly of the head of bacteriophage T4. *Nature* **227:**680–685

Lanius, R.A., Pasqualotto, B.A., Shaw, C.A. 1993. γ-Aminobutyric $acid_A$ receptor regulation by a chloride-dependent kinase and a sodium-dependent phosphatase. *Mol. Brain Res.* **20:**192–198

Laurie, D.J., Wisden, W., Seeburg, P.H. 1992. The distribution of thirteen $GABA_A$ receptor subunit mRNAs in the rat brain. III. embryonic and postnatal development. *J. Neurosci.* **12,11:**4151–4172

Leidenheimer, N.J., Browning, M.D., Harris, R.A. 1991. $GABA_A$ receptor phosphorylation: multiple sites, actions and artifacts. *TIPS* **12:**84–87

Levitan, E.S., Blair, L.A.C., Dionne, V.E., Barnard, E.A. 1988. Biophysical and pharmacological properties of cloned $GABA_A$ receptor subunits expressed in *Xenopus* oocytes. *Neuron* **1:**773–781

Licari, P., Bailey, J.E. 1991. Factors influencing recombinant protein yields in an insect cell-baculovirus expression system: multiplicity of infection and intracellular protein degradation. *Biotechnol. Bioeng.* **37:**238–246

McDonald, B.J., Moss, S.J. 1994. Differential phosphorylation of intracellular domains of γ-Aminobutyric acid type A receptor subunits by calcium/calmodulin type 2-dependent protein kinase and cGMP-dependent protein kinase. *J. Biol. Chem.* **269:**18111–18117

Miller, L.K. 1988. Baculoviruses as gene expression vectors. *Annu. Rev. Microbiol.* **42:**177–199

Moss, S.J., Smart, T.G., Blackstone, G.D., Huganir, R.L. 1992. Functional modulation of $GABA_A$ receptors by cAMP-dependent protein phosphorylation. *Science* **257:**661–665

Oh, D.J., Dichter, M.A. 1988. Desensitization of GABA-induced currents in cultured rat hippocampal neurons. *Neuroscience* **49:**571–576

Porter, N.M., Angelotti, T.P., Twyman, R.E., MacDonald, R.L. 1992. Kinetic properties of $alpha_1$ $beta_1$ gamma-aminobutyric acidA receptor channels expressed in Chinese hamster ovary cells: regulation by pentobarbital and picrotoxin. *Mol. Pharmacol.* **42:**872–881

Porter, N.M., Twyman, R.E., Uhler, M.D., MacDonald, R.L. 1990. Cyclic AMP-dependent protein kinase decreases $GABA_A$ receptor current in mouse spinal neurons. *Neuron* **5:**789–796

Sambrook, J., Fritsch, E.F., Maniatis, T. 1989. Molecular Cloning. Laboratory Manual. Cold Spring Harbor Laboratory Press, New York

Schönrock, B., Bormann, J. 1993. Functional heterogeneity of hippocampal $GABA_A$ receptors. *Eur. J. Neurosci.* **5:**1042–1049

Sigel, E., Baur, R., Malherbe, P. 1991. Activation of protein kinase C results in down-modulation of different recombinant $GABA_A$-channels. *FEBS Lett.* **291:**150–152

Sigel, E., Baur, R., Trube, G., Möhler, H., Malherbe, P. 1990. The effect of subunit composition of rat brain $GABA_A$ receptors on channel function. *Neuron* **5:**703–711

Sivilotti, L., Nistri, A. 1991. GABA receptor mechanisms in the central nervous system. *Prog. Neurobiol.* **36:**35–92

Summers, M.D., Smith, G.E. 1988. A Manual of Methods for Baculovirus Vectors and Insect Cell Culture Procedures. Texas Agric. Exp. Station Bull. 1555: 1–57

Taylor, J.W., Ott, J., Eckstein, F. 1985. The rapid generation of oligonucleotide-directed mutations at high frequency using phosphorothioate-modified DNA. *Nucleic Acids Res.* **13:**8765–8785

Towbin, H., Staehelin, T., Gordon, J. 1979. Electrophoretic transfer of proteins from polyacrylamide gels to nitrocellulose sheets: procedure and some applications. *Proc. Natl. Acad. Sci. USA* **76:**4350–4354

Twyman, R., Green, R.M., MacDonald, R.L. 1992. Kinetics of open channel block by penicillin of single $GABA_A$ receptor channels from mouse spinal cord neurones in culture. *J. Physiol.* **445:**97–127

Verdoorn, T.A., Draguhn, A., Ymer, S., Seeburg, P.H., Sakmann, B. 1990. Functional properties of recombinant rat $GABA_A$ receptors depend upon subunit composition. *Neuron* **4:**919–928

Vyklicky, L. Jr., Benveniste, M., Mayer, M.L. 1990. Modulation of *N*-methyl-d-aspartic acid receptor desensitization by glycine in mouse cultured hippocampal neurones. *J. Physiol.* **428:**313–331

Yoon, K-W. 1994. Voltage-dependent modulation of $GABA_A$ receptor channel desensitization in rat hippocampal neurons. *J. Neurophysiol.* **71:**2151–2160

Yoon, K-W., Covey, D.F., Rothman, S.M. 1993. Multiple mechanisms of picrotoxin block of GABA-induced currents in rat hippocampal neurons. *J. Physiol.* **464:**423–439

Zorumski, C.F.MD., Isenberg, K.E.MD. 1991. Insights into the structure and function of GABA-benzodiazepine receptors: ion channels and psychiatry. *Am. J. Psychiatry* **148:**162–173